

Alkylation of biphenyl with propylene using MCM-22 and ITQ-2 zeolites

J. Aguilar^{a,*}, S.B.C. Pergher^b, C. Detoni^b, A. Corma^c, F.V. Melo^c, E. Sastre^d

^a Universidad Autónoma Metropolitana, División de Ciencias Básicas e Ingeniería, Av. San Pablo 180, 02200 México D.F., Mexico

^b Universidade Integrada do Alto Uruguai e das Missões, Campus Erechim, Departamento de Química, Av. Sete de Setembro 1621, 99700-000 Erechim, RS, Brazil

^c Instituto de Tecnología Química, UPV-CSIC, Avenida de los Naranjos s/n, 46022 Valencia, Spain

^d Instituto de Catálisis y Petroleoquímica, CSIC, C/Marie Curie, 2. Cantoblanco, 28049 Madrid, Spain

Available online 22 January 2008

Abstract

Alkylation of biphenyl with propylene in gas phase was carried out over two zeolites: MCM-22 and ITQ-2. The influence of zeolite structure on reaction activity and selectivity is discussed.

The alkylation activity follows the order: ITQ-2 > MCM-22. The influence of the change in the morphology in MCM-22 to ITQ-2 has been studied and it has been observed that, under the reaction conditions used here, the reaction takes place mainly on the external surface, which indicates that the dimensions of 10 MR channels inhibit the diffusion of the bulky reactants inside the zeolitic pores and, also, explains the high *o*-IPBP selectivity observed.

© 2007 Elsevier B.V. All rights reserved.

Keywords: MCM-22; ITQ-2; Alkylation of biphenyl; Propylene; Shape selectivity; Activity

1. Introduction

The Friedel–Crafts alkylation of aromatics using zeolites has been extensively studied from basic and applied points of view in order to introduce functional groups in aromatic hydrocarbons [1–5]. More specifically, the alkylation of biphenyl with propylene is a reaction of practical interest since it may produce 4,4'-diisopropylbiphenyl (4,4'-DIPB) [6–18] an important intermediate in the preparation of thermotropic polymers of use in liquid crystal manufacture [19,20].

In a previous study [21] we reported the use of different zeolites in the alkylation of biphenyl with propylene, observing that the alkylation activity follows the order: Y > Beta > MCM22 > ZSM-5. MCM-22 zeolite showed a very high selectivity to *ortho*-isopropylbiphenyl (*o*-IPBP), higher than that obtained with Y zeolite. MCM-22 [22–25] is one of the most interesting zeolite structures synthesized up to now. It consists of two-independent pore systems, one formed by two-dimensional

sinusoidal channels, and the other by large supercages having an inner diameter of approximately 0.71 nm and height of 1.82 nm. Both channel systems are accessible through 10 member ring (10 MR) openings. It is very difficult to think that *o*-IPBP formed in supercages can be passed through these windows. Then, the formation of *o*-IPBP in this zeolite has to be limited to the active sites in external surface.

Recently a new material named ITQ-2 [26–30] has been prepared by swelling and delaminating a MWW precursor. In this way a solid formed by very thin sheets (approximately 2.5 nm high) with an extremely high external surface area ($\geq 700 \text{ m}^2/\text{g}$) was produced. These sheets consist of a hexagonal array of cups that penetrate into the sheet from both sides. These cups would have an aperture of approximately 0.7 nm, formed by a 12-member ring (12 MR). The cups, which are 0.7 nm deep, meet at the center of the layer forming a double 6-MR window that connects the cups, bottom to bottom. As result, a smooth 10-MR channel system runs around the cups, inside the sheet.

In the present work, we compare the activity and selectivity of MCM-22 and ITQ-2 zeolites in the alkylation of biphenyl with propylene in gas phase.

* Corresponding author.

E-mail address: apj@correo.azc.uam.mx (J. Aguilar).

2. Experimental

2.1. Zeolite synthesis

The layered MCM-22 (P) precursor was prepared using hexamethylenimine (HMI) (Aldrich), silica (Aerosil 200, Degussa), sodium aluminate (56% Al_2O_3 , 37% Na_2O , Carlo Erba), sodium aluminate (Prolabo), and deionized water. More specifically, a sample with $\text{Si}/\text{Al} = 50$ was prepared in the following way: NaAlO_2 (0.234 g) and NaOH (0.816 g) were dissolved in 103.45 g of H_2O , and then, 6.358 g of HMI and 7.689 g of SiO_2 were added to this solution while stirring. After 30 min of stirring the resulting gel was introduced into a 60-mL PTFE lined stainless-steel autoclave, rotate at 60 rpm, and heated at 408 K for 11 days. The chemical composition of the final gel was $\text{SiO}_2/\text{Al}_2\text{O}_3 = 100$; $\text{OH}/\text{SiO}_2 = 0.10$; $\text{Na}/\text{SiO}_2 = 0.18$. After quenching the autoclaves in cold water, the samples were centrifuged at 12,000 rpm, washed thoroughly with deionized water until pH of <9.0 was reached, and subsequently dried at <333 K, overnight. A portion of this MCM-22 (P) was calcined in air at 853 K for 3 h giving MCM-22 [22]. Another portion was delaminated to generate the corresponding ITQ-2 [29].

The ITQ-2 sample was obtained by swelling the precursor with hexadecyltrimethylammonium bromide. Typically 27 g of precursor was mixed with 105 g of an aqueous solution of 29 wt% surfactant and 33 g of an aqueous solution of 40 wt% tetrapropylammonium hydroxide and refluxed for 16 h at 353 K. The completion of swelling can be monitored by (XRD), which shows an increase in the distance between the layers from 2.7 nm to approximately 4.5 nm. The layers are forced apart by placing the slurry in an ultrasound bath (50 W, 40 kHz) for 1 h. Subsequent addition of a few drops of concentrated hydrochloric acid, until the pH is below 2, allows harvesting of the solids by centrifuging. Then,

removal of organic material by calcination at 853 K yields ITQ-2 [26].

The acid form of both zeolites was obtained by carrying out three times the NH_4^+ exchange (NH_4Cl , 2.5 mol/L, 353 K, 1 h) and calcinations (823 K for 3 h).

2.2. Catalyst characterization

X-ray diffraction measurements were performed on a Philips X'PERT with automatic slits using $\text{Cu K}\alpha$ radiation. IR spectra were obtained in a Nicolet 710 FTIR by using a Pyrex vacuum cell (CaF_2 windows) and self-supported wafers of 10 mg cm^{-2} . For acidity measurements, the samples were previously degassed at 673 K in vacuum (10^{-3} Pa) overnight (background spectrum). Then pyridine (6×10^2 Pa) was admitted at room temperature and degassed at 423, 523, and 673 K for 1 h. After each treatment spectra were recorded at room temperature and the background subtracted. Absorption isotherms of N_2 and Ar were obtained on an apparatus ASAP 2000 after pretreating the samples under vacuum at 673 K overnight.

2.3. Reaction

The alkylation of biphenyl with propylene was carried out in a continuous, fixed bed, glass tubular reactor electrically heated. The temperature of reaction was 523 K. Biphenyl was diluted in heptane (20%) and the mixture was fed into the reactor together with propylene, being the ratio of biphenyl to propylene of 4 mol mol^{-1} . Samples of reaction products were collected at different times on stream, and analyzed by gas chromatography. The contact time between reactants and catalyst was varied by changing the amount of catalyst and maintaining constant the flow of feed (1.36 mol/h of biphenyl).

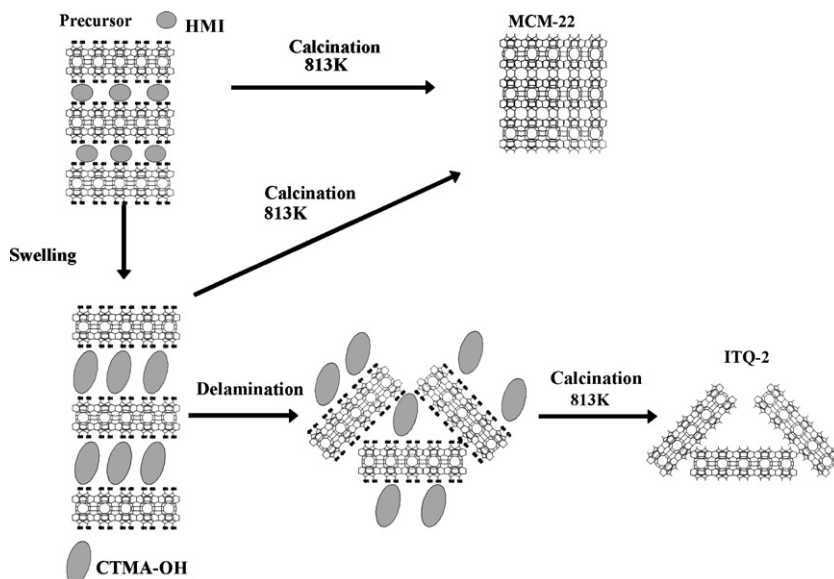


Fig. 1. Scheme for the preparation of the MCM-22 and ITQ-2 obtained from the MCM-22 precursor.

Table 1

Specific surface area and volume of the different samples from nitrogen adsorption isotherms

Sample	S_{BET} (m ² /g)	S_{micro} (m ² /g)	S_{ext} (m ² /g)	V_{total} (cm ³ /g)	V_{micro} (cm ³ /g)	V_{BJH} (cm ³ /g)
MCM-22	451	355	96	0.524	0.177	0.169
ITQ-2	841	45	796	0.948	0.017	0.853

 $S_{\text{ext}} = S_{\text{BET}} - S_{\text{micro}}$. V_{BJH} : volume of pores from 17 to 300 Å.

3. Results and discussion

3.1. Zeolite synthesis

The different types of structures formed, starting from the laminar precursor, are schematized in Fig. 1. It can be seen that while in the case of MCM-22 the large 1.8×0.7 nm 12 MR cavities are present, these should be absent in ITQ-2. Furthermore, it can also be seen that the external surface of individual layers of MWW structures leave half-open 12 MR cavities, which we call “cups” arranged in a regular array of approximately $0.7 \text{ nm} \times 0.7 \text{ nm}$ cups. A further look to Fig. 1, allow us to conclude that the highest possible amount of accessible cups will be obtained if a successful delamination of the laminar precursor was achieved.

We have recently shown this possibility by swelling the precursor with CTMA⁺ [29]. The XRD patterns of the different samples obtained by these modifications of the as-made MCM-22 are presented in Fig. 2. When the swelled precursor was dispersed in water, as it has been described in Section 2, it becomes delaminated and the resultant product (ITQ-2) appears almost amorphous to the X-ray. Indeed, ITQ-2 does not show the 0 0 1 peak with its 2.5 nm periodicity characteristic of a MWW topology. Comparing the XRD pattern of ITQ-2 with that of MWW-type zeolite, it can be seen that the high angle peaks are broader for ITQ-2, which is indicative of a reduction in the size of the crystal. In other words, delamination has significantly reduced the long-range order in the new material.

The N₂ adsorption isotherm data are indicative of an increase of total surface area and pore volume with the delamination process, as can be seen in Table 1, where the

Table 2

Acidity measurements by pyridine adsorption IR spectroscopy

Sample	423 K		523 K		623 K	
	Lewis	Brönsted	Lewis	Brönsted	Lewis	Brönsted
MCM-22	16.0	29.0	13.0	19.0	12.0	7.0
ITQ-2	17.4	13.6	16.2	11.8	10.8	4.7

values of total surface area and volume, as well as that of mesoporous (1.7–30 nm) area and volume, are summarized.

From the Ar isotherms values (not shown), a Horvath–Kawazoe [26] type of representation has been performed and those data confirm the presence of micropores that still exist in ITQ-2.

Previous studies of IR spectra of the MCM-22 and ITQ-2 [28], show that a larger number of SiOH groups (bands at 3745 and 960 cm^{-1}) are present on ITQ-2, as it should be if a delamination of the layered precursor has occurred. Meanwhile, the spectroscopic results in the hydroxyl region show that a decrease in the total number of acidic hydroxyl groups has occurred during delamination, probably due to the occurrence of a certain degree of dealumination. This should be reflected in the total number of Brönsted acid sites, as is indeed shown by the pyridine adsorption results presented in Table 2, where it can be observed that a decrease in Brönsted acidity has occurred during delamination.

However, from the point of view of the reaction of large reactant molecules, the important parameter is not the total Brönsted acidity but the number of acid sites accessible to the reactant. In order to discuss this, we have also carried out the adsorption of 2,6-diterbutylpyridine (2,6-DTBP) which

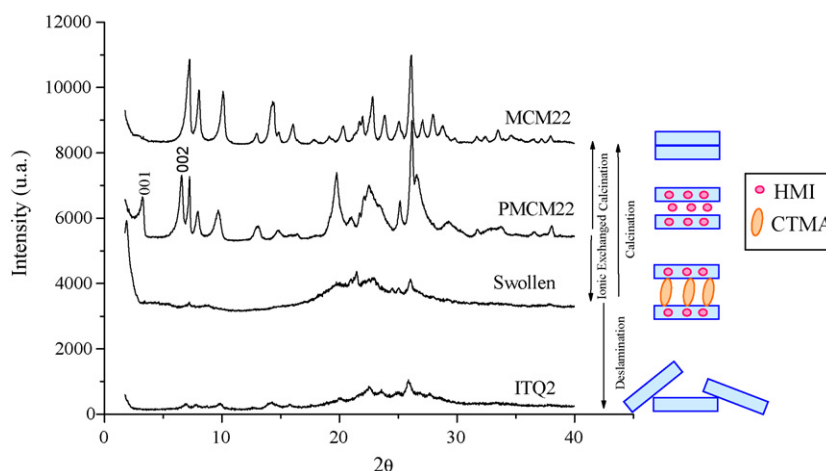


Fig. 2. X-ray diffraction patterns of the MCM-22 (P) and its derivatives.

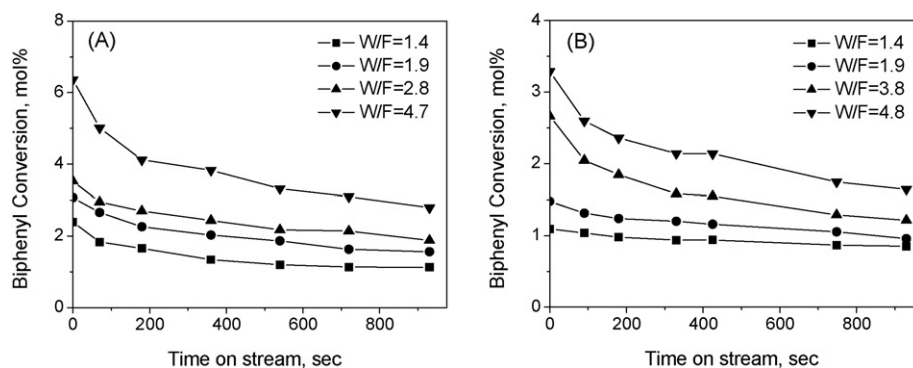


Fig. 3. Total conversion vs. time on stream in the alkylation of biphenyl with propylene at 523 K and different contact times on ITQ-2 (A) and H-MCM-22 (B) zeolites.

certainly cannot access into circular 10 MR channels and, consequently, should only measure the amount of Brönsted acid sites accessible through the external surface, i.e., through the cups. When the acids sites measured with 2,6DTBPy are compared with the total number of acid sites as measured by the pyridine, it can be seen that a much larger number of external acid sites (~ 4 times higher) are present in ITQ-2 than in MCM-22 [26]. This again supports the hypothesis that delamination process is increasing not only the external surface area but also the number of the Brönsted acid sites accessible to large molecules.

3.2. Catalytic results

During the experiments carried out with the different catalysts in the alkylation of biphenyl with propylene, the activity decrease with time on stream on all the catalysts studied due to the formation of coke on the catalysts surface, similarly as it occurred during the gas phase catalytic alkylation of biphenyl with methanol with different zeolites [31]. In order to compare the catalytic activity of the samples in absence of deactivation, the biphenyl conversion at zero time reaction was estimated from the values of conversion obtained at different times on stream and fitting these conversions to the following equation:

$$x_t = x_0 \exp[-k_d t^{0.5}] \quad (1)$$

where x_0 is the conversion at zero time on stream, x_t is the conversion at a given t time on stream and k_d is a decay constant. In Fig. 3 are plotted some experimental data showing the conversion of biphenyl versus the reaction time, obtained with the ITQ-2 and MCM-22 catalysts by using different contact times at 523 K. In all cases a good fitting of Eq. (1) to the experimental data has been observed.

The reaction was followed at different contact times for each catalyst samples, and from the results obtained under differential reactor conditions at zero time on stream the initial reaction rates were calculated, like we had reported in previous papers [21,31]. These values together with the decay constant are shown in Table 3. As can be seen in this table, while the calculated deactivation constants change, in some

cases, with total conversion, it is possible nevertheless to establish that MCM-22 and ITQ-2 have similar deactivation. It can be seen that there is not a direct correlation between deactivation rate and catalytic activity.

3.3. Catalytic selectivity

The yields to the different products obtained in the reaction of alkylation of biphenyl have also been extrapolated at zero time on stream in order to avoid the possible influence of catalyst deactivation on selectivity. As expected, the main primary products observed are: *o*-, *m*- and *p*-isopropylbiphenyls (IPBP), while diisopropyl-biphenyls (DIPB) appear as secondary products on all catalysts. No other products than IPBP or DIPB were detected with our analytical system.

The influence of total conversion on the reaction product selectivities for both catalysts is shown in Fig. 4. In this Figure, the selectivities to *o*-, *m*-, and *p*-IPBP are referred to the total yield of monoalkylated products. In all cases, the selectivities of the three monoalkylated biphenyls do not change with total conversion. Otherwise, the selectivity to DIPB increases with total conversion as can be expected for a secondary reaction.

The presence of 10 member ring (10 MR) channels or windows introduces strong constraints for biphenyl to diffuse into the channels. Then, it is assumed that with ZSM-5 and MWW structures, only the external surface will be active for carrying out the reaction.

The selectivities obtained with these catalysts, at the same level of conversion, are compared in Table 4 with another large pore zeolite with faujasite structure [21]. It can be observed that both zeolites, MCM22 and ITQ2, present a higher selectivity towards the *o*-IPBP isomer compared with the results obtained with the HY zeolite. This can be due to diffusional limitations

Table 3
Deactivation constant and reaction rate for the reaction at 523 K

Catalyst	Total conversion (%) ^a	$k_d \times 10^3$ (s ^{-1/2}) ^b	Reaction rate (mol/gh)
H-MCM-22	1–3	12–26	0.0077
ITQ-2	2–6	27	0.0170

^a Experimental range of biphenyl conversion (molar %).

^b Range of calculated deactivation constants.

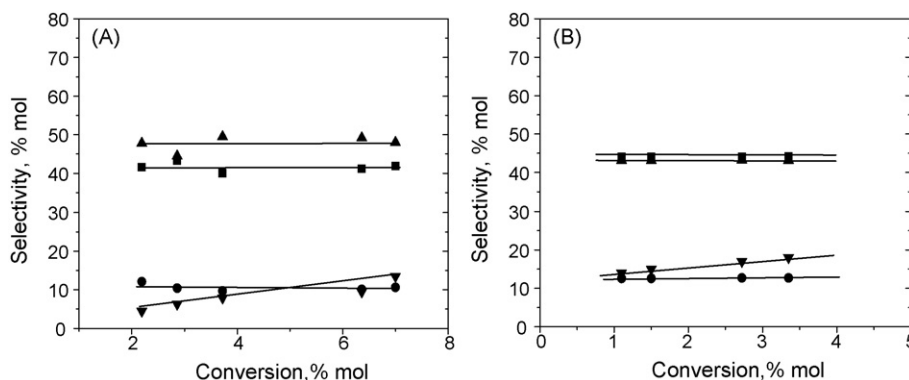


Fig. 4. Selectivity of *o*-IPBP (●), *m*-IPBP (▲), *p*-IPBP (■) and DIPB (▼) vs. total conversion in the alkylation of biphenyl with propene at 523 K. (A) ITQ-2 sample and (B) H-MCM-22 sample.

Table 4
Selectivity of reaction products ($T = 523$ K, biphenyl conversion $\sim 4\%$)

Catalyst	Product selectivities (mol%)				
	IPBP	DIPB	<i>o</i> -IPBP	<i>m</i> -IPBP	<i>p</i> -IPBP
H-MCM-22	82.0	18.0	12.7	43.1	44.2
ITQ-2	89.8	10.2	10.6	47.8	41.6
HY(PQ)-1	94.8	5.2	3.1	62.5	34.4

which hindered the access of the biphenyl molecules inside the pores of the narrower MCM-22 and ITQ-2 zeolites. So, the formation of the bulky *o*-IPBP isomer should take place on the acid sites located in the external surface, which are not sterically limited.

This hypothesis can also explain the observed differences in activity for these two zeolites, which can be attributed to the different crystal sizes and corresponding external surface areas of the two zeolites. The catalytic activity could seem very high supposing that the reaction mainly occurs on the external surface area. If it is so, these zeolites may have a considerable external surface area, and it can be possible taking into account the structures of these zeolites. Roque-Malherbe et al. [32,33] studied the diffusion of aromatic hydrocarbons in several zeolites. In the case of MCM-22 zeolite they found two superimposed processes (one very rapid and the other very slow) in the diffusion of a bulky molecule as *o*-xylene, and they attributed the rapid diffusion of *o*-xylene to the presence of the truncated cavities on the external crystal face in the (0 0 1) direction. Then, a significant amount of active sites, but no selective sites, can be directly accessible to the reactants, being responsible to the higher DIPB selectivity and the distribution of the monoalkylated isomers for these zeolites.

4. Conclusions

The reaction of alkylation of biphenyl with propylene has been studied on the MCM-22 and ITQ-1 microporous zeolites. The catalytic activity of the reaction follows the order: ITQ-2 > H-MCM-22. This reaction is catalyzed by strong Brönsted acid sites (which retain adsorbed pyridine at desorption temperature of 623 K or higher). The catalytic activity and selectivity of the studied zeolites can be explained taking into

account the zeolite structure and the accessibility of molecules. However, ITQ-2 and H-MCM-22 zeolites show high selectivities towards *o*-IPBP and DIPBs, which cannot be explained by their pore structures.

The reaction of alkylation of biphenyl with propylene on zeolites can be considered a clean reaction to obtain only alkylated products, without other lateral reactions, and it can be used as a test reaction to characterize large and medium pore zeolites. It is important to compare catalytic activity and selectivity in absence of deactivation to be sure to obtain the appropriate values.

Acknowledgement

Authors thank the funds provided by the CNPq (Brazil)/CONACYT (México) Researchers Exchange Program.

References

- [1] S. Csicsery, *Zeolites* 4 (1984) 203.
- [2] Y. Sugi, M. Toba, *Catal. Today* 19 (1994) 187.
- [3] P.B. Venuto, *Micropor. Mater.* 2 (1994) 297.
- [4] A. Corma, *Chem. Rev.* 95 (1995) 559.
- [5] A. Corma, H. García, *Catal. Today* 38 (1997) 257.
- [6] Y. Sugi, T. Matsuzaki, T. Hanaoka, K. Takeuchi, T. Tokoro, G. Takeuchi, *Stud. Surf. Sci. Catal.* 60 (1991) 303.
- [7] X. Tu, M. Matsumoto, T. Matsuzaki, T. Hanaoka, Y. Kubota, J.H. Kim, Y. Sugi, *Catal. Lett.* 21 (1993) 71.
- [8] Y. Sugi, X.-L. Tu, T. Matsuzaki, T. Hanaoka, Y. Kubota, J.H. Kim, M. Matsumoto, K. Nakajima, A. Igarashi, *Catal. Today* 31 (1996) 3.
- [9] M. Matsumoto, X. Tu, T. Matsuzaki, T. Hanaoka, Y. Kubota, Y. Sugi, J.H. Kim, K. Nakajima, A. Igarashi, K. Kunimori, *Stud. Surf. Sci. Catal.* 105 (1997) 1317.
- [10] T. Matsuda, T. Urata, U. Saito, E. Kikuchi, *Appl. Catal. A: Gen.* 131 (1995) 215.
- [11] D. Vergani, R. Pris, H.W. Kouwenhoeven, *Appl. Catal. A: Gen.* 163 (1997) 71.
- [12] T. Matsuda, E. Kikuchi, *Stud. Surf. Sci. Catal.* 83 (1994) 295.
- [13] Y. Sugi, T. Matsuzaki, T. Hanaoka, Y. Kubota, J.H. Kim, X.L. Tu, M. Matsumoto, *Catal. Lett.* 26 (1994) 181.
- [14] T. Hanaoka, K. Nakajima, Y. Sugi, T. Matsuzaki, Y. Kubota, S. Tawada, K. Kunimori, A. Igarashi, *Catal. Lett.* 50 (1998) 149.
- [15] G.S. Lee, J.J. Maj, S.C. Roake, J.M. Garcés, *Catal. Lett.* 2 (1989) 243.
- [16] T. Matsuda, T. Urata, E. Kikuchi, *Appl. Catal. A: Gen.* 123 (1995) 205.
- [17] Y. Sugi, T. Matsuzaki, T. Hanaoka, Y. Kubota, J.H. Kim, X.L. Tu, M. Matsumoto, *Catal. Lett.* 27 (1994) 315.

- [18] T. Matsuda, T. Kimura, E. Herawati, C. Kobayashi, E. Kikuchi, *Appl. Catal. A: Gen.* 136 (1996) 19.
- [19] C. Song, H.H. Schobert, *Fuel Process. Technol.* 34 (1993) 157.
- [20] C. Song, H.H. Schobert, *Am. Chem. Soc. Div. Fuel Chem. Prep.* 40 (1995) 249.
- [21] J. Aguilar, A. Corma, F.V. Melo, E. Sastre, *Catal. Today* 55 (2000) 225.
- [22] S.B.C. Pergher, A. Corma, V. Fornés, *Quim. Nova* 26 (2003) 795.
- [23] M.K. Rubin, P. Chu, US Patent 4,954,325 (1990).
- [24] M.E. Leonowicz, J.A. Lawton, S.L. Lawton, M.K. Rubin, *Science* 264 (1994) (1910).
- [25] R. Milini, G. Perego, W.O. Parker Jr., G. Bellusi, L. Carluccio, *Micropor. Mesopor. Mater.* 4 (1995) 221.
- [26] S.B.C. Pergher, PhD Thesis, Universidad Politécnica de Valencia, Spain, 1997.
- [27] A. Corma, V. Fornés, J.M. Guil, J. Martínez-Triguero, S.B.C. Pergher, Th.L.M. Maessen, J.G. Buglass, *Micropor. Mesopor. Mater.* 38 (2000) 301.
- [28] A. Corma, V. Fornés, J. Martínez-Triguero, S.B.C. Pergher, *J. Catal.* 186 (1999) 57.
- [29] A. Corma, V. Fornés, S.B.C. Pergher, Th.T.M. Maessen, J.G. Buglass, *Nature* 396 (1998) 353.
- [30] S.B.C. Pergher, A. Corma, V. Fornés, Abstracts of the XVIII Simposio Iberoamericano de Catálisis, Porlamar (Venezuela), 2002, p. 1308.
- [31] J. Aguilar, F.V. Melo, E. Sastre, *Appl. Catal. A: Gen.* 175 (1998) 181.
- [32] G. Sastre, N. Raj, C. Richard, C. Catlow, R. Roque-Malherbe, A. Corma, *J. Phys. Chem. B* 102 (1998) 3198.
- [33] R. Roque-Malherbe, R. Wendelbo, A. Mifsud, A. Corma, *J. Phys. Chem. B* 99 (1995) 14064.